International Conference on Computational Methods in Marine Engineering
MARINE 2011
L.Eça, E. Oñate, J. García, T. Kvamsdal and P. Bergan (Eds)

# A NUMERICAL MODEL TO DETERMINE SHIP MANOEUVRING MOTION IN REGULAR WAVES

**JOCHEN SCHOOP-ZIPFEL AND MOUSTAFA ABDEL-MAKSOUD**

Institute of Fluid Dynamics and Ship Theory (FDS)
Hamburg University of Technology
Schwarzenbergstr. 95C, 21073 Hamburg, Germany
e-mail: jochen.schoop@tu-harburg.de, www.tu-harburg.de/fds

**Key words:** Manoeuvring, Seakeeping, Impulse-Response, Time-Domain

**Abstract.** A numerical program for time-domain calculations of the manoeuvring behaviour in regular waves is presented. The program is based on frequency-dependent coefficients, transfered to time-domain by using the impulse response function. Memory effects are included by using the convolution integral. Nonlinear effects are accounted for by adjusting the mass, the damping, and the restoring data to the instantaneous floating condition. The equations of motion are solved in six degrees of freedom. The forces of the manoeuvring motion are calculated with the nonlinear slender-body theory. The resistance, propulsion and rudder forces follow from semi-empirical procedures. For the wave excitation, Froude-Krylov and diffraction forces are regarded. A validation of the described procedure is performed for manoeuvring in calm water and straight-ahead motion in regular head waves.

## NOMENCLATURE

| | | | |
|---|---|---|---|
| $\underline{\underline{a}}(\omega)$ | frequency-dependent added mass | $D$ | draft of ship |
| | | $Fn$ | Froude number of ship |
| $\underline{\underline{A}}$ | infinite-frequency added mass | $I_{xy}, I_{xz}, I_{yz}$ | products of inertia |
| $\underline{\underline{b}}(\omega)$ | frequency-dependent damping | $J$ | propeller advance coefficient |
| $\underline{\underline{B}}(\tau)$ | retardation function | $k_T$ | thrust coefficient |
| $B$ | beam of ship | $L_{pp}$ | length between perpendiculars |
| $c_B$ | block coefficient of ship | $m$ | mass of ship |
| $c_{F0}$ | skin friction resistance coefficient | $t$ | time |
| | | $u, v, p, r$ | velocity in surge, sway, roll and yaw direction |
| $c_M$ | midship coefficient | | |
| $\underline{\underline{C}}$ | restoring matrix | $\underline{X}$ | external force vector |
| $d$ | draft of ship section | $\underline{x}, \underline{\dot{x}}, \underline{\ddot{x}}$ | state position, velocity and |

| | | | |
|---|---|---|---|
| | acceleration vectors | | of added mass per section |
| $x_G, y_G, z_G$ | coordinates of center of gravity | $\mu$ | added mass per section |
| $X, Y, K, N$ | external force in surge, sway, | $\omega$ | motion frequency |
| | roll and yaw direction | $\rho$ | density of water |
| $z_y$ | z-coordinate of point of attack | $\tau$ | time-integrand |

## 1 INTRODUCTION

Simulating ship manoeuvres is typically carried out for calm water conditions. Sea waves may lead to a strong change of the hydrodynamic forces acting on the ship and thus effect the manoeuvring performance.

However, some difficulties are arising by combining manoeuvring theory and seakeeping theory. This is mainly due to the fact that hydrodynamic forces of different natures dominate. In seakeeping, the inertia forces dominate, while manoeuvring forces are dominated by viscosity-related effects.

For first estimations in the design stage of a ship or for the optimisation of the ship motion behaviour, a time efficient computation is necessary. For seakeeping purposes, this can be obtained by potential strip theory in frequency-domain. Simulations in time-domain give the opportunity to extend the motions to large amplitudes and to consider nonlinear forces. The consideration of the instantaneous floating condition, i.e. the instantaneous waterline, allows the investigation of the motions of hull forms with large changes in the hull form near the waterline, such as flared bows, overhanging sterns, etc.

An overview on numerical methods for the calculation of combined manoeuvring and seakeeping is given in [1]; on behalf of the International Towing Tank Conference (ITTC) investigations showed the capability of different numerical methods.

The problem of combining manoeuvring theory and seakeeping theory can be attacked from the manoeuvring or the seakeeping point of view. Sutulo and Soares [2] developed a model for the simulation of manoeuvring in waves coming from the seakeeping theory. To improve the manoeuvring performance, the still-water manoeuvring forces that are calculated with their model are subtracted, and forces from an experiment-based manoeuvring model are added. Their preliminary results are encouraging; the ship's reaction to waves is in accordance with expectations.

Umeda et al developed a model where the focus lies on broaching prediction [3]. An improved prediction accuracy for ship motions in following and quartering seas was demonstrated by considering second-order terms of waves, like effects on hull manoeuvring coefficients, hydrodynamic lift due to wave fluid velocity and the change in added mass due to relative wave elevations [4].

A unified model based on a modular concept was developed by Skejic and Faltinsen [5] by adopting a two-time scale formulation. The usage of second-order wave loads and the manoeuvring concept of Söding [6] yield results that have been extensively verified and validated. It was demonstrated that the incident waves may have an important influence on the manoeuvring behaviour of a ship.

Ayaz et al [7] developed a nonlinear coupled 6DOF numerical model with frequency dependent coefficients, incorporating memory effects and random waves. The axes system accounts for extreme motions. The numerical results indicate that the inclusion of frequency coefficients definitely affects the accuracy of the predictions.

The feasibility and the advantage in accounting nonlinear terms over linear theory has also been shown by Pereira [8]. He developed the nonlinear strip theory code SIMBEL, where the pressure is integrated over the instantaneous wetted surface. Memory effects are also taken into account.

Only a few experiments on manoeuvring in waves have been published. Ueno et al [9] presented the results of straight running, turning, zig-zag and stopping tests with a VLCC model ship in regular waves.

The present study presents a numerical program for time-domain calculations of the manoeuvring behaviour in waves, called MoeWe (Manoevring in Waves). The program is based on frequency-dependent coefficients, transfered to time-domain by using the impulse response function proposed by Cummins [10]. Memory effects are included by using the convolution integral. Nonlinear effects are accounted for by adjusting the mass, the damping and the restoring data to the instantaneous floating condition.

## 2 COORDINATE SYSTEM

The coordinate systems are set up from a manoeuvring view. Three different coordinate systems are introduced:

1. Global coordinates are used to describe the track of the ship. This earth-fixed frame is defined by $O_0x_0y_0z_0$, with $O_0$ being an arbitrary origin, $x_0$ and $y_0$ lying on the undisturbed free surface, and $z_0$ pointing downwards.

2. The body axes $Cxyz$ are linked to the ship treated as a rigid body. The origin $C$ is placed at the keel at midship section. $x$ is pointing to the bow, while $y$ points to starbord and $z$ downwards. At the initial time moment $t = 0$, the body fixed frame coincides with the earth frame.

3. The ship motion components are described in body semi-fixed axes (horizontal axes) $O\xi\eta\zeta$. This system moves with the forward speed of the ship but is not involved in the heave, pitch and roll motion. I.e., it does not follow the periodic ship motions. Velocities, accelerations and external actions are referenced to this coordinate system. In this system, the equations are solved and integrated.

## 3 EQUATION OF MOTION

The mathematical model is based on the impulse response function. With this approach, the hydrodynamic reaction forces and moments due to time-varying ship motions can be described.

### 3.1 Impulse response function

Cummins [10] showed that the hydrodynamic force (in the following, the moments are also ment when talking about forces) can be written as:

$$\underline{F} = \underline{\underline{A}} \cdot \underline{\ddot{x}}(t) + \int_{-\infty}^{t} \underline{\underline{B}}(t-\tau) \cdot \underline{\dot{x}}(t) \cdot d\tau \tag{1}$$

The equation of motion in time-domain is based on Newton's second law. The hydrodynamic force together with a linear restoring term $\underline{\underline{C}} \cdot \underline{x}$ and an external load $\underline{X}(t)$ yields:

$$(\underline{\underline{M}} + \underline{\underline{A}}) \cdot \underline{\ddot{x}}(t) + \int_{0}^{\infty} \underline{\underline{B}}(\tau) \cdot \underline{\dot{x}}(t-\tau) \cdot d\tau + \underline{\underline{C}} \cdot \underline{x}(t) = \underline{X}(t) \tag{2}$$

The added mass $\underline{\underline{A}}$ and damping $\underline{\underline{B}}$ in equation 2 are independent from the motion frequency but can be simply expressed in terms of the frequency-dependent added mass and damping data, following the approach of Ogilvie [11]. By comparing the equations in frequency- and in time-domain and an inverse Fourier Transform, the desired function $\underline{\underline{B}}(\tau)$ yields:

$$\underline{\underline{B}}(\tau) = \frac{2}{\pi} \cdot \int_{0}^{\infty} \underline{\underline{b}}(\omega) \cdot \cos(\omega\tau) \cdot d\omega \tag{3}$$

The expression for the mass term is valid for any value of $\omega$ and thus also for $\omega = \infty$; this provides:

$$\underline{\underline{A}} = \underline{\underline{a}}(\omega = \infty) \tag{4}$$

A more detailled description of this derivation can be found in [12].

The left hand side of equation 2 is still linear. The external force $\underline{X}(t)$ on the right-hand side of the equation can also contain nonlinear terms.

The coefficients in this equation ($\underline{\underline{A}}$, $\underline{\underline{B}}$, $\underline{\underline{C}}$) depend on the state of the body, i.e. the instantaneous floating condition, here described by $\underline{x}$. To be able to handle bodies with large motions and hence with different state vectors $\underline{x}$, this is set as a variable, yielding

$$(\underline{\underline{M}} + \underline{\underline{A}}(\underline{x}(t))) \cdot \underline{\ddot{x}}(t) + \int_{0}^{\infty} \underline{\underline{B}}(\underline{x}(t), \tau) \cdot \underline{\dot{x}}(t-\tau) \cdot d\tau + \underline{\underline{C}}(\underline{x}(t)) \cdot \underline{x}(t) = \underline{X}(t) \tag{5}$$

where $\underline{\underline{B}}$ also depends on past states.

The equation is numerically treated by the Runge-Kutta method.

### 3.2 Coefficient determination

For the determination of the frequency dependent, linear hydrodynamic mass and damping as well as of the linear restoring PDStrip is used, [13]. PDStrip computes the seakeeping behaviour of ships and other floating bodies according to the strip method. It is mainly confined to linear responses, but it takes into account a few nonlinear effect.

The hydrodynamic coefficients are determined for a predefined set of different floating conditions, which are characterized by forward speed, draft, trim and heel.

### 3.3 External forces

The right-hand side of equation 5 consists of external forces acting on the system. These forces can contain nonlinear parts. The right-hand side contains forces due to the manoeuvring motion, resistance and propulsion forces, rudder forces and forces due to exciting waves. Moreover, the forces arising from the coordinate transformation to the body semi-fixed axes $O\xi\eta\zeta$, e.g. centrifugal and corriolis forces, are passed to the right-hand side. Since the program is built up modular, these parts can easily be changed or additional parts can be introduced.

Manoeuvring motions are dominated by velocity dependent forces; so an accurate description of these forces is of high relevance. Furthermore, the model shall be kept as simple as possible. The forces due to manoeuvring motion are calculated with the slender-body theory according to [6]. The basis of this approach is the idea that the hull force in $y$-direction on a strip of length $dx$ is equal to the change in time of the $y$-momentum of the water that is next to the hull at this strip. The amount of this water is the added mass of the certain hull section ($\mu$). For manoeuvring motion, the added mass for zero frequency has to be used. This is also calculated with PDStrip for each section of the ship.

For the manoeuvring motion only four degrees of freedom are relevant, i.e. surge, sway, roll and yaw.

The transverse momentum of the water per shiplength follows subsequently to $\mu(v+xr)$. The substantial derivative yields the force per length:

$$\begin{pmatrix} X \\ Y \\ K \\ N \end{pmatrix} = \int_L \begin{pmatrix} 0 \\ 1 \\ 1 \\ x \end{pmatrix} (-\frac{\partial}{\partial t} + u\frac{\partial}{\partial x}) \left[ \begin{pmatrix} 0 \\ \mu \\ -z_y\mu \\ \mu \end{pmatrix} (v + xr) \right] dx \tag{6}$$

The minus sign is neccessary because it is not the force of the ship on the water that is considered, but rather, the force of the water on the ship.

The first part of this equation, i.e. the terms including $\frac{\partial}{\partial t}$, is already considered on the left-hand side of equation 5. The second part is added to the external force. On this part, some corrections are applied following [6]. Furthermore, a nonlinear force calculated with the stagnation pressure, the area and the drag coefficient is introduced:

$$\begin{pmatrix} X \\ Y \\ K \\ N \end{pmatrix} = \frac{1}{2}\rho \int_L \begin{pmatrix} 0 \\ -1 \\ z_D \\ -x \end{pmatrix} (v + xr)\,|v + xr|\,C_D\,d\,dx \tag{7}$$

The basis for the estimation of the resistance of the ship need to be model experiments or extensive CFD-calculations. The resistance is calculated as the sum of the residual resistance $R_R$ and the skin friction resistance $R_{F0}$. The residual resistance has to be

obtained by model tests or CFD-calculations. The skin friction resistance coefficient can be calculated with the ITTC 1957 formula:

$$c_{F0} = \frac{0.075}{(log_{10}Rn - 2)^2} \tag{8}$$

The thrust is determined with the known open water characteristics of the propeller. The thrust coefficient $k_T$ is approximated as a straight line depending on the advance coefficient $J$.

Rudder forces are calculated as proposed in [6]. The lift, drag and moment coefficients are approximated with semi-empirical formulas. The incident flow at the rudder is computed with the propeller slipstream theory. The consequential rudder lift and drag are diminished due to the finite lateral extent of the propeller slipstream.

For the wave excitation, Froude-Krylov and diffraction forces are regarded. The former is due to the pressure field in the undisturbed wave. The latter is the force that arises because the ship changes the pressure field. Both are linear forces.

The forces are calculated with PDStrip in six degrees of freedom for a predefined set of wave frequencies and floating conditions. They are stored in a database as a function of encounter frequency, heave displacement, pitch and roll angle. Depending on the wave frequency and the instantaneous floating condition in the time-domain calculation, the wave excitation forces are available.

When transforming the velocities and accelerations from the earth-fixed frame to the body semi-fixed frame, some nonlinear terms arise:

$$X = -mrv - mr^2x_G + 2mprz_G \tag{9}$$

$$Y = mru - mr^2y_G \tag{10}$$

$$Z = 0 \tag{11}$$

$$K = -mruz_G + I_{yz}r^2 \tag{12}$$

$$M = -z_Gmrv - I_{xz}r^2 + 2z_G^2mpr \tag{13}$$

$$N = mx_Gur + mrvy_G + I_{xy}r^2 - I_{yz}2pr \tag{14}$$

## 4 VALIDATION

The validation of the predescribed procedure (MoeWe) is split in two parts. First, standard maneuvers on calm water are calculated and compared to results from model experiments. Second, the motions of a ship with steady forward speed in head waves are investigated.

### 4.1 Manoeuvring in calm water

For the validation of the manoeuvring prediction, model experiment data from the SIMMAN workshop 2008 [14] are taken. At this workshop, four different ships were investigated and different numerical methods as well as experimental results were compared and published.

In the present study, standard manoeuvres are simulated with a KVLCC1 tanker ship and a KCS container ship. The KVLCC1 is a 300 K tanker ship with bulb bow and stern, see Figure 1a. It has barge type stern frame-lines with a fine stern end bulb, i.e. relatively V-shaped frame-lines. The KCS is a modern Container ship specially designed for testing and validation purposes, see Figures 1b and 1c. It has a bulbous bow and stern. Both ship models have no bilge keels. So two ships are chosen that are likely to have different manoeuvring charateristics. A comparison of the results with the model experimental data is made.

(a) KVLCC1 (b) KCS bow view (c) KCS stern view

Figure 1: Ship hulls and discretised frames for manoeuvring validation

Figure 2 shows the results of a 10°/10° and a 20°/20° zig-zag maneuver for the KVLCC1. The analogue results for the KCS are plotted in Figure 3. The blue line represents the calculated heading of the ship as a function of time. The respective rudder angle is plotted in red. The green and the purple line show the results of model tests.

As can be seen from the figures, there is good agreement between calculated and measured results.

### 4.2 Straight motion in head waves

Two different ship types are calculated in head waves: a Wigley hull and the S-175 container ship. Experimental data for comparison is taken from Journée [15] and the proceedings of ITTC 1978 [16]. Journée performed model experiments with four different Wigley hulls in head waves. In the ITTC proceedings, experimental data for a S-175 container ship are presented.

In the present study, calculations are conducted with the Wigley hull IV, a hull with a amidship section coefficient of $c_M = 0.6667$ and a length to breadth ratio of $L/B = 5$.

Results in the frequency-domain are obtained with the strip method PDStrip. The calculated response amplitude operator (RAO) in heave and pitch are shown in Figure 4, for Froude numbers of $Fn = 0.2$ and $Fn = 0.3$. The calculated results are plotted with dashed lines, while the experimental results are marked with crosses. A good agreement can be seen for the heave motion, while the results of the pitch motion show a significant

deviation in the encounter frequency range of $\omega_e = 1.2...1.8$, where a clear resonance peak is seen in the experimental results. However, the experimental values seem to be very high.

Subsequently, the added mass and damping terms are transformed with the impulse response function, and calculations in time-domain are conducted. For validation purposes, calculations with regular waves with different frequencies are performed. The calculated results are used to recalculate the RAOs for heave and pitch motion. These results are compared with the numerical results of PDStrip, see Figure 5. The case with zero forward speed is also considered. The numerical results show that the transformation of calculated motions from the frequency-domain into time-domain yields no errors for zero forward speed. However, differences arise with increasing forward speed, as can be seen in the figure. The resonance peaks are less pronounced in time-domain. Reasons for this are under investigation.

Like the Wigley hull, similar results can be found for the S-175; however, there is a good agreement of the pitch RAO calculated with PDStrip and the experimental data, as seen in Figure 6. The differences between the calculation results again increase with increasing forward speed, see Figure 7.

## 5 CONCLUSIONS

A time-domain method using convolution integral formulation is presented and applied to predict zig-zag manoeuvres for a KCS container ship and a KVLCC1 tanker, and to predict heave and pitch motion for a Wigley hull and a S-175 container ship in regular head waves. Diverse additional forces account for external effects acting on the ship.

The calculated zig-zag manoeuvres show good agreement with experimental data. Good agreement can also be found for the RAO in heave of the Wigley hull and the RAO in heave and pitch of the S-175 ship calculated in frequency-domain. The calculations in time-domain with zero forward speed correlate almost perfectly with the frequency-domain, while differences arise with increasing forward speed. So far, the source for these differences couldn't be determined.

Due to short computational times, this program represents a good method for quick estimations of ship motion behaviour and optimisation purposes.

The validation that has been conducted so far is limited to linear responses, only small wave amplitudes have been chosen. To validate the nonlinear behaviour of the code, further calculations with larger wave amplitudes should be performed and compared to corresponding experiments.

Moreover, the combined manoeuvring and seakeeping behaviour shall be validated, i.e. calculations and experiments of standard manoeuvres in waves need to be carried out.

## REFERENCES

[1] D. Vassalos et al., "The specialist committee for the prediction of extreme motions

and capsizing -final report and recommendations of the 23rd ITTC," *Proceedings of 23rd International Towing Tank Conference*, vol. 23, pp. 611–649, 2002.

[2] S. Sutulo and C. G. Soares, "A unified nonlinear mathematical model for simulating ship manoeuvring and seakeeping in regular waves," in *Marsim*, 2006.

[3] N. Umeda and M. R. Renilson, *Manoeuvring and Control of Marine Craft*, ch. Broaching - A Dynamic Analysis of Yaw Behaviour of a Vessel in a Following Sea, pp. 533–543. Computational Mechanics Publication, 1992. pp. 533-543.

[4] N. Umeda, H. Hashimoto, and A. Matsuda, "Broaching prediction in the light of an enhanced mathematical model, with higher-order terms tanken into account," *Journal of Marine Science and Technology*, vol. 7, pp. 145–155, Januar 2003.

[5] R. Skejic and O. M. Faltinsen, "A unified seakeeping and maneuvering analysis of ships in regular waves," *Journal of Marine Science and Technology*, vol. 13, pp. 371–394, 2008.

[6] H. Söding, "Bewertung der Manövriereigenschaften im Entwurfsstadium," *Jahrbuch der Schiffbautechnischen Gesellschaft*, vol. 78, pp. 179–204, 1984. in German.

[7] Z. Ayaz, D. Vassalos, and K. J. Spyrou, "Manoeuvring behaviour of ships in extreme astern seas," *Ocean Engineering*, vol. 33, pp. 2381–2434, 2006.

[8] R. Pereira, "Simulation nichtlinearer Seegangslasten," *Ship Technology Research*, vol. 35, pp. 173–193, 1988. in German.

[9] M. Ueno, T. Nimura, and H. Miyazaki, "Experimental study on manoeuvring motion of a ship in waves," in *Marsim*, 2003.

[10] W. E. Cummins, "The impulse response function and ship motions," *Schiffstechnik*, vol. 47, no. 9, pp. 101–109, 1962.

[11] T. Ogilvie, "Recent progress towards the understanding and prediction of ship motions," *Proc. 5th Symposium on Naval Hydrodynamics*, 1964.

[12] J. Journée and W. Massie, *Offshore Hydromechanics*. Delft University of Technology, 2001.

[13] H. Söding and V. Bertram, *Program PDSTRIP: Public Domain Strip Method*, August 2007. http://pdstrip.sourceforge.net/.

[14] F. Stern and K. Agdrup, eds., *Workshop on Verification and Validation of Ship Manoeuvring Simulation Methods, SIMMAN*, FORCE Technology, 2008.

[15] J. Journée, "Experiments and calculations on 4 wigley hull forms in head waves," Tech. Rep. 0909, Delft University of Technology, 1992.

[16] *Proceedings of the 15th ITTC*, (The Hague, The Netherlands), May 1978.

Table 2: Main particulars of ships for validation

| | **KVLCC1** | **KCS** | **Wigley** | **S-175** |
|---|---|---|---|---|
| **Main particulars** | | | | |
| $L_{pp}$ (m) | 320.0 | 230.0 | 40 | 175 |
| $B$ (m) | 58.0 | 32.2 | 8 | 25.4 |
| $D$ (m) | 20.8 | 10.8 | 2.5 | 9.5 |
| $m$ (m3) | 312738 | 52030 | 370 | 24742 |
| $C_B$ | 0.8101 | 0.651 | - | 0.6 |
| $C_M$ | 0.9980 | 0.985 | 0.6667 | - |
| $x_G$ (m) | 11.1 | -3.4 | 0 | -2.5 |
| $Fn$ | 0.142 | 0.26 | 0.2; 0.3 | 0.275 |

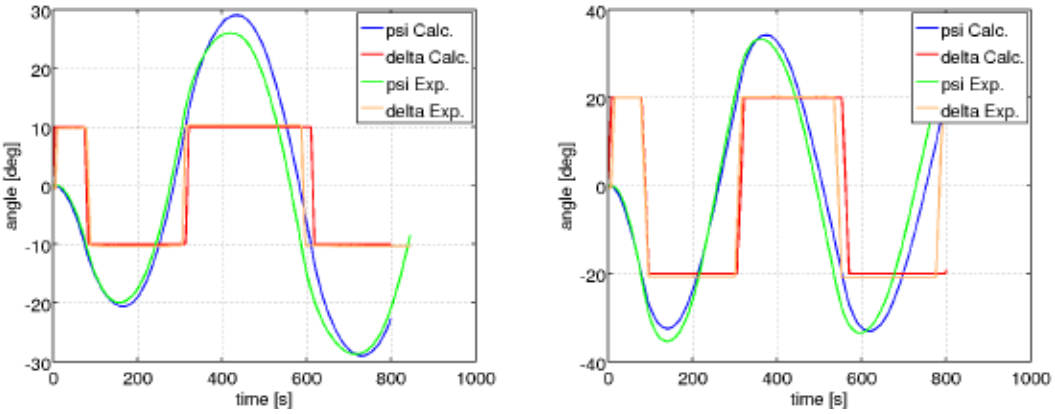


Figure 2: Zig-zag manoeuvre of KVLCC1 (left: 10°/10°, right: 20°/20°)

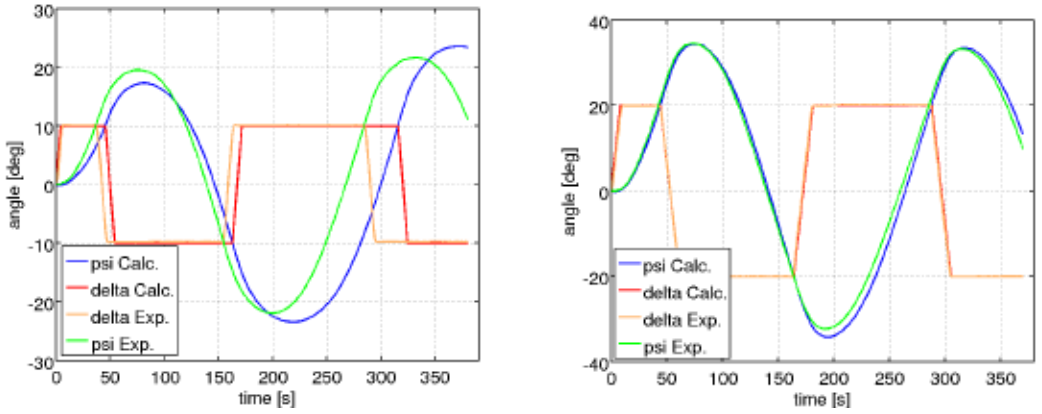


Figure 3: Zig-zag manoeuvre of KCS (left: 10°/10°, right: 20°/20°)

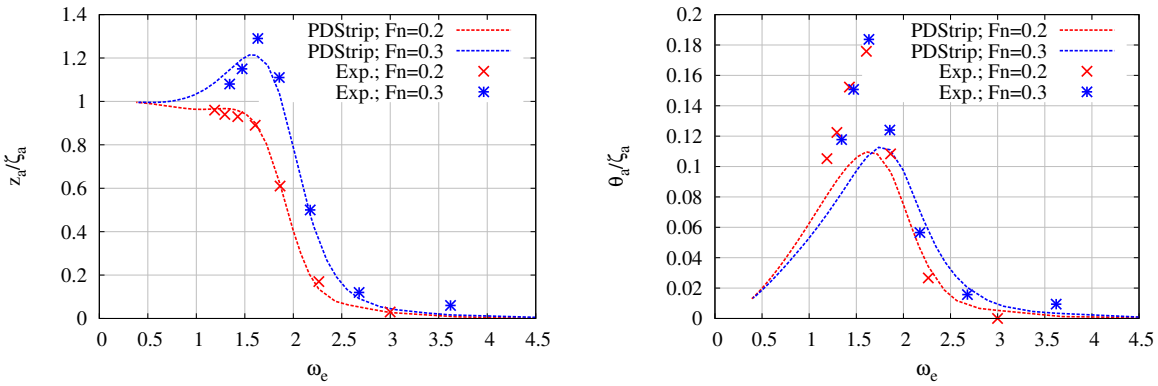


Figure 4: RAO of Wigley; PDStrip vs. experiment (left: heave, right: pitch)

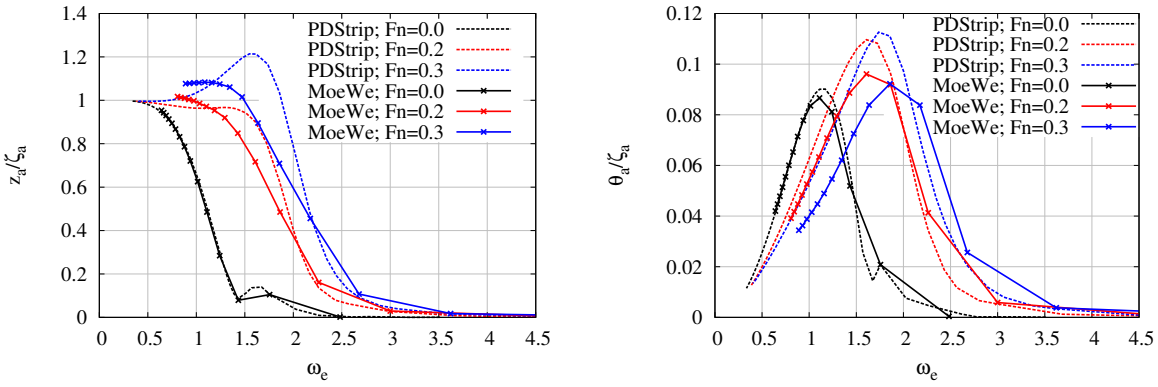


Figure 5: RAO of Wigley; MoeWe vs. PDStrip (left: heave, right: pitch)

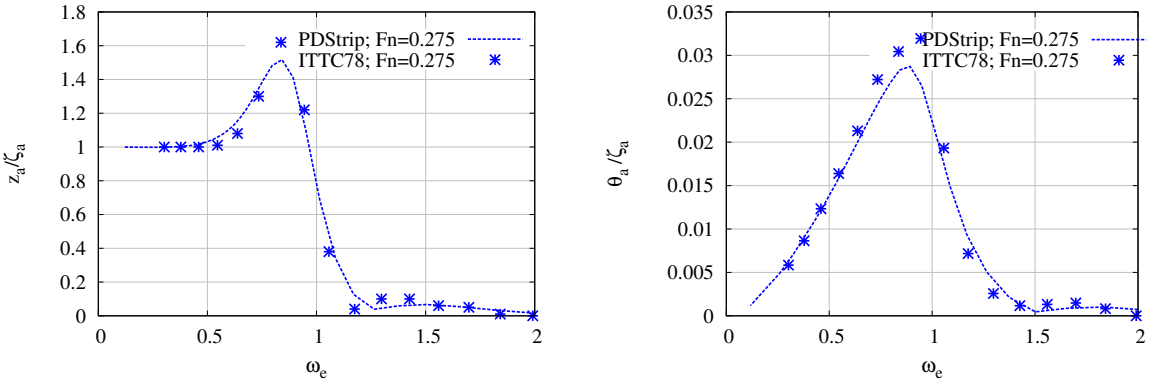


Figure 6: RAO of S-175; PDStrip vs. experiment (left: heave, right: pitch)

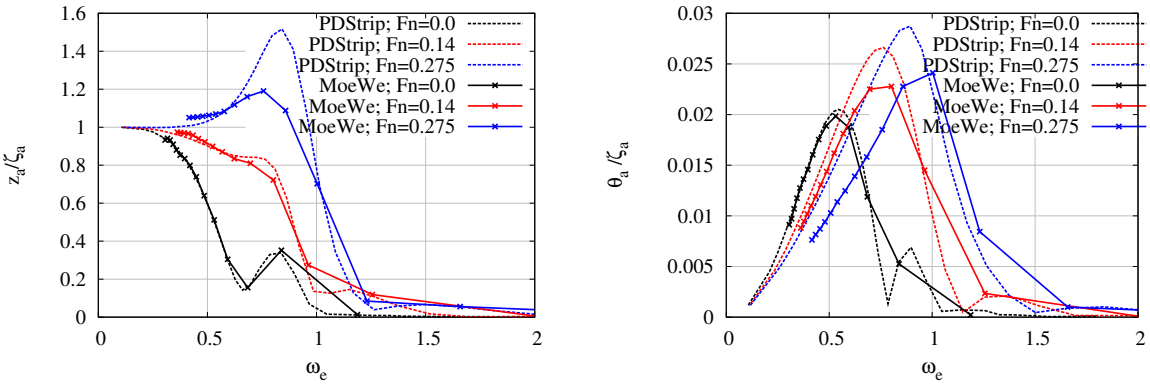


Figure 7: RAO of S-175; MoeWe vs. PDStrip (left: heave, right: pitch)